Supplement of

Quantification of the Role of Stabilized Criegee Intermediates in the Formation of Aerosols in Limonene Ozonolysis

Y. W. Gong and Z. M. Chen

Correspondence to: Z. M. Chen (zmchen@pku.edu.cn)

Chemicals used in this study

This study used the following: R-(+)-Limonene (Sigma-Aldrich, $\geq$ 99.0 %), 2-butanol (Sigma-Aldrich, $\geq$ 99.5 %), acetic acid (Sigma-Aldrich, $\geq$ 99.7%), ultrapure water (18MΩ, Millipore), N_2 ($\geq$ 99.999 %, Beijing Haikeyuanchuang Practical Gas Company Limited, Beijing, China), O_2 ($\geq$ 99.999 %, Beijing Haikeyuanchuang Practical Gas Company Limited, Beijing, China).

The wall loss fraction of SOA mass concentration

The wall loss fraction of SOA mass concentration is calculated as Eq. (S1):

$$F_{wall\ loss} = ([In] - [Out])/[In] \qquad (S1)$$

where $F_{wall\ loss}$ is the wall loss fraction of SOA mass concentration, [In] and [Out] are the SOA mass concentrations at the inlet and outlet of the reactor. Wall loss fractions at different relative humidity (RH) are shown in Table S1.

Calculating the amount of SCIs consumed by water

Here the amount of SCIs consumed by water could not be derived directly, and it was

calculated through the reaction rate ratio of SCIs reaction with water and AA as Eqs.

(S2) and (S3):

$$\frac{SCI_{H2O}}{SCI_{AA}} = \frac{k_{(SCI+H2O)I} \cdot [H_2O] \cdot SCI_I}{k_{(SCI+AA)} \cdot [AA] \cdot SCI_{Total}} \tag{S2}$$

$$SCI_{H2O} = \frac{k_{(SCI+H2O)I} \cdot [H_2O] \cdot 0.545}{k_{(SCI+AA)} \cdot [AA]} \cdot \Delta AA \tag{S3}$$

where SCI_{H2O} (molecule cm^{-3}) is the amount of SCIs reacted with H_2O; SCI_{AA}

(molecule cm^{-3}) is the amount of SCIs reacted with AA; $k_{(SCI+H2O)I}$ (cm^3 molecule^{-1}

s^{-1}) is the rate constant of SCI_I reaction with H_2O; $k_{(SCI+AA)}$ (cm^3 molecule^{-1} s^{-1}) is the

rate constant of SCIs reaction with AA; $[H_2O]$ (molecule cm^{-3}) is the concentration of

H_2O; $[AA]$ (molecule cm^{-3}) is the concentration of AA; SCI_I (molecule cm^{-3}) is the

amount of SCI_I generated; SCI_{Total} (molecule cm^{-3}) is the amount of total SCIs

generated; ΔAA (molecule cm^{-3}) is the amount of AA consumed.

SCI_I reaction with H_2O and $(H_2O)_2$

To acquire the reaction rate ratio of SCIs reaction with water and AA, it should be

figured out whether the reaction with H_2O or $(H_2O)_2$ dominants in SCI_I reaction with

water. This problem was discussed by estimating the generation of H_2O_2, which is a

major product formed from SCI_I reaction with water (Hasson et al., 2001;

Winterhalter et al., 2000). The dependence of H_2O_2 yield on RH reported in our

previous study is shown in Fig. S2 (Gong et al., 2018), we estimated the formation of

H_2O_2 based on SCI_I reaction with H_2O and SCI_I reaction with $(H_2O)_2$, respectively.

The inferred relationships between H_2O_2 and the concentrations of H_2O and $(H_2O)_2$

are shown as Eqs. (S4)–(S7):

$$\frac{SCI_{H2O}}{SCI_I} = \frac{\Delta H_2O_2}{SCI_I} = \frac{k_{(SCI+H2O)I} \cdot [H_2O]}{k_{(SCI+H2O)I} \cdot [H_2O] + k_{(other)I}} \tag{S4}$$

$$\Delta H_2O_2 = \frac{1}{1 + \dfrac{k_{(other)I}}{k_{(SCI+H2O)I} \cdot [H_2O]}} \cdot SCI_I \tag{S5}$$

$$\frac{SCI_{(H2O)2}}{SCI_I} = \frac{\Delta H_2O_2}{SCI_I} = \frac{k_{(SCI+(H2O)2)I} \cdot [(H_2O)_2]}{k_{(SCI+(H2O)2)I} \cdot [(H_2O)_2] + k_{(other)I}} \tag{S6}$$

$$\Delta H_2O_2 = \frac{1}{1 + \dfrac{k_{(other)I}}{k_{(SCI+(H2O)2)I} \cdot [(H_2O)_2]}} \cdot SCIs_I \tag{S7}$$

where SCI_{H2O} (molecule cm^{-3}) is the amount of SCIs reacted with H_2O; SCI_I

(molecule cm^{-3}) is the amount of SCI_I generated; ΔH_2O_2 (molecule cm^{-3}) is the

amount of H_2O_2 generated; $[H_2O]$ (molecule cm^{-3}) is the concentration of H_2O;

$[(H_2O)_2]$ (molecule cm^{-3}) is the concentration of $(H_2O)_2$; $k_{(SCI+H2O)I}$ (cm^3 molecule^{-1}

s^{-1}) is the rate constant of SCI_I reaction with H_2O; $k_{(SCI+(H2O)2)I}$ (cm^3 molecule^{-1} s^{-1}) is

the rate constant of SCI_I reaction with $(H_2O)_2$; $k_{(other)I} = k_{(isomerization)I} +$

$k_{(SCI+products)I} \cdot$ [products], meaning that $k_{(other)I}$ accounts for the sum of SCI_I

isomerization and reaction with other products in the system. In Fig. S2, the red line

represents the estimated yield of H_2O_2 based on SCI_I reaction with H_2O when

$k_{(SCI+H2O)I}$ is set as 5×10^{-16} cm^3 molecule^{-1} s^{-1} and $k_{(other)I}$ is 30 s^{-1}; the green line

represents the estimated yield of H_2O_2 based on SCI_I reaction with $(H_2O)_2$ when

$k_{(SCI+(H2O)2)I}$ is set as 1×10^{-12} cm^3 molecule^{-1} s^{-1} and $k_{(other)I}$ is 30 s^{-1}. The estimation

based on SCI$_I$ reaction with H$_2$O showed a better fitting with the measured results and k$_{(SCI+H2O)I}$ was used to calculate the amount of SCIs reacted with water.

Calculating the amount of exocyclic double bonds (exo-DB) ozonated in bulk phase

Here the second-generation oxidation at 80% RH was analyzed. Results showed that at 80% RH the amount of exo-DB ozonated was ~ 15 ppbv larger than that under dry condition. Assuming that particles at 80% RH were liquid and exo-DB were ozonated in bulk phase, the amount of exo-DB ozonated in bulk phase could be calculated according to Eq. (S8):

$$\Delta[DB_{(aq)}] = k_{(aq)} \cdot [O_{3(aq)}] \cdot [DB_{(aq)}] \cdot t \qquad (S8)$$

where $\Delta[DB_{(aq)}]$ (mol L^{-1}) is the amount of exo-DB ozonated in bulk phase; $k_{(aq)}$ (L mol^{-1} s^{-1}) is the rate constant of exo-DB ozonated in bulk phase; $[O_{3(aq)}]$ (mol L^{-1}) is the concentration of O$_3$ in bulk phase; $[DB_{(aq)}]$ (mol L^{-1}) is the concentration of exo-DB in bulk phase; t (s) is the reaction time. During the reaction, although bulk-phase exo-DB and O$_3$ were consumed, gas-phase O$_3$ and SVOCs containing exo-DB would constantly enter bulk phase, and it was hypothesized that both of $[O_{3(aq)}]$ and $[DB_{(aq)}]$ could maintain stable during reaction. Based on measurement results, the average SOA mass concentration in the second-generation oxidation was around 50 μg m^{-3}, and $\Delta[DB_{(aq)}]$ was derived to be 15.94 mol L^{-1}. $[O_{3(aq)}]$ was calculated through Henry's law as Eq. (S9):

$$H_{O3} = \frac{\left[O_{3(aq)}\right]}{P_{O3}} \qquad (S9)$$

where H_{O3} (mol L^{-1} Pa^{-1}) is the Henry's law constant of O_3, which is 9.28×10^{-8} mol

L^{-1} Pa^{-1} at 298 K (Sander, 2015); P_{O3} (Pa) is the partial pressure of O_3 in the gas

phase. It was calculated that $[O_{3(aq)}]$ was 1.10×10^{-7} mol L^{-1}, and the rate constant of

unsaturated first-generation oxidation products ozonated in aqueous phase was

reported to be about 4.0×10^4 L mol^{-1} s^{-1}(Witkowski et al., 2018a, b), according to

which $[DB_{(aq)}]$ was derived to be 15.09 mol L^{-1}. Assuming that the molecular weight

of unsaturated first-generation products was 200 g mol^{-1}, the density of those

particulate unsaturated compounds was 3.02 g cm^{-3}, which was even larger than the

aerosol density of 1.30 g cm^{-3}, suggesting that bulk-phase ozonolysis was not able to

explain the large amount of exo-DB ozonated under high-humidity conditions.

Estimating the uptake coefficient of unsaturated first-generation products on

aqueous aerosols

Here the second-generation oxidation at 80% RH was analyzed. The uptake

coefficient of unsaturated first-generation products can be estimated when simplifying

the heterogeneous reaction as a pseudo-first-order reaction using Eq. (S10)

(Ravishankara, 1997):

$$\gamma = \frac{4k}{\omega A} \qquad (S10)$$

where γ is the uptake coefficient of unsaturated products; k (s^{-1}) is the rate constant of pseudo-first-order reaction; ω (m s^{-1}) is the mean molecular velocity; A (m^2 m^{-3}) is the total surface area concentration of particles. ω is calculated using Eq. (S11):

$$\omega = \sqrt{\frac{8RT}{\pi M_x}} \tag{S11}$$

where R (J mol^{-1} K^{-1}) is the gas constant; T (K) is the absolute temperature; M_x (kg mol^{-1}) is the molar weight of unsaturated first-generation products, which is assumed to be 0.2 kg mol^{-1} and ω is derived as 178 m s^{-1}. During the second-generation oxidation the amount of exo-DB ozonated through heterogeneous reaction at 80% RH was around 15 ppbv, and since the heterogeneous reaction process here was treated as a pseudo-first-order reaction, k could be calculated through Eq. (S12):

$$\Delta[DB] = k \cdot [O_3] \cdot t \tag{S12}$$

where $\Delta[DB]$ (molecule cm^{-3}) is the amount of exo-DB ozonated through heterogeneous reaction; $[O_3]$ (molecule cm^{-3}) is the concentration of O_3; t (s) is the reaction time. O_3 concentration in the second-generation oxidation was 11.9 ppmv and the reaction time was 240 s, so k was calculated to be 5.25×10^{-6} s^{-1}. The surface area concentration of aerosols in the second-generation oxidation was estimated to be $\sim 4 \times 10^{-5}$ m^2 m^{-3}, and γ was derived to be 2.95×10^{-3}.

SOA formation in the first-generation oxidation

Growth curves of SOA mass concentration and SOA yield in the first-generation oxidation are shown in Fig. S4. It is noted that the SOA growth curve at certain RH is

similar to the curve at the adjacent RH, and for instance, SOA growth curves of 10% and 20% RH are similar with each other. The same situation is observed between conditions of 30% and 40% RH, and SOA growth above 60% RH seems unchanged with RH increasing. To better identify SOA growth curves at different RH in the picture, conditions of < 0.5%, 10%, 30%, 50%, 70%, and 90% RH are chosen to show.

Estimating the amount of SCIs scavenged by excess AA

When adding excess AA (10.0 ± 0.4 ppmv) into the reaction system, the amount of SCIs consumed by AA could be estimated as Eq. (S13):

$$\frac{SCI_{AA}}{SCI} = \frac{k_{(SCI+AA)} \cdot [AA]}{k_{(SCI+H2O)} \cdot [H_2O] + k_{(other)}} \tag{S13}$$

where SCI_{AA} (molecule cm^{-3}) is the amount of SCIs reacted with AA; SCI (molecule cm^{-3}) is the amount of SCI generated; [AA] (molecule cm^{-3}) is the concentration of AA; [H$_2$O] (molecule cm^{-3}) is the concentration of H$_2$O; $k_{(SCI+AA)}$ (cm^3 molecule^{-1} s^{-1}) is the rate constant of SCI reaction with AA; $k_{(SCI+H2O)}$ (cm^3 molecule^{-1} s^{-1}) is the rate constant of SCI reaction with H$_2$O; $k_{(other)} = k_{(isomerization)I} + k_{(SCI+products)} \cdot$ [products], meaning that $k_{(other)}$ accounts for the sum of SCI isomerization and reaction with other products in the system. Using the parameters derived in the study, reactions of SCI$_I$ and SCI$_{II}$ were both considered and it was calculated that even under 90% RH the concentration of AA used was sufficient for scavenging more than 99% of SCIs generated during reactions.

The fraction of SCIs converting into SOA (α_{SCI})

The slope of the fitting line of SOA versus SCIs represents the amount of SOA contributed by per unit concentration of SCIs, which is denoted as SOA_{perSCI}. When taking the average of the slopes in the first- and second-generation oxidations, SOA_{perSCI} under dry and low-humidity conditions was calculated to be 1.39 μg m^{-3}, and under high-humidity conditions SOA_{perSCI} was 2.46 μg m^{-3}. In theory, if all SCIs could convert into SOA by producing low-volatile products, of which the molar mass was assumed to be 200 g mol^{-1}, it was estimated that SOA_{perSCI} was 8.17 μg m^{-3}. As the molar mass of products formed from monoterpene-derived SCIs was expected to be large (Lee and Kamens, 2005), SOA_{perSCI} was calculated to be 12.26 μg m^{-3} when assuming the molar mass of the products was 300 g mol^{-1}. It was derived that under dry and low-humidity conditions α_{SCI} was 11–17% and under high-humidity conditions α_{SCI} was 20–30%.

The amount of SOA formed from SCIs reaction could be estimated as Eqs. (S14) and (S15) when assuming the molar weight of low-volatile products formed from SCIs is 300 g mol^{-1}:

$$SOA_{SCI} = \alpha_{SCI} \cdot SCI \cdot \frac{1}{N_A} \cdot 3 \times 10^{14} \qquad (S14)$$

$$SOA_{SCI} = 5 \times 10^{-10} \alpha_{SCI} \cdot SCI \qquad (S15)$$

where SOA_{SCI} (μg m^{-3}) is the mass concentration of SOA formed from SCIs reaction; SCI (molecule cm^{-3}) is the amount of SCIs in reaction system; α_{SCI} is the conversion rate of SCIs that are valid for SOA formation; N_A (6.02 × 10^{23} molecule mol^{-1}) is the

Avogadro constant. When water exists, SCI at different RH could be calculated as Eqs. (S16) and (S17):

$$SCI = SCI_{Total} - \frac{1}{1 + \frac{k_{(other)\mathrm{I}}}{k_{(SCIs+H2O)\mathrm{I}} \cdot [H_2O]}} \cdot SCIs_{\mathrm{I}} \qquad (S16)$$

$$SCI = SCI_{Total} - \frac{RH}{RH + 7.8} \cdot SCI_{\mathrm{I}} \qquad (S17)$$

where RH (%) is the relative humidity.

Figure caption

Table S1. Wall loss fractions of SOA mass concentration at different relative humidity (RH).

Table S2. The amounts of SCIs (molecule cm^{-3}) under different concentrations of acetic acid (AA, molecule cm^{-3}) and different relative humidity (RH) in the first-generation oxidation.

Table S3. The amounts of SCIs (molecule cm^{-3}) under different concentrations of acetic acid (AA, molecule cm^{-3}) and different relative humidity (RH) in the second-generation oxidation.

Table S4. The reactants concentrations (ppbv) in calculations of steady-state concentrations of SCIs in forest, urban area, and indoor area.

Figure S1. Diagram of the thermostatic coil collector.

Figure S2. The dependence of the molar yield of hydrogen peroxide (H_2O_2) on relative humidity (RH).

Figure S3. The variation of the consumption of acetic acid (ΔAA) with the concentration of acetic acid ([AA]) at different relative humidity (RH) in the second-generation oxidation.

Figure S4. Growth curves of (a) SOA mass concentration (SOA) and (b) SOA yield (Y) versus limonene reacted (ΔHC) at different relative humidity (RH) in the first-generation oxidation.

Figure S5. Growth curves of (a) SOA mass concentration (SOA) and (b) SOA yield (Y) versus reaction time at different relative humidity (RH) in the second-generation oxidation.

Figure S6. The variation of SOA mass concentration (SOA) with the concentration of acetic acid ([AA]) at different relative humidity (RH) in the second-generation oxidation.

References

Boy, M., Mogensen, D., Smolander, S., Zhou, L., Nieminen, T., Paasonen, P., Plass-Dülmer, C., Sipilä, M., Petäjä, T., Mauldin, L., Berresheim, H., and Kulmala, M.: Oxidation of SO_2 by stabilized Criegee intermediate (sCI) radicals as a crucial source for atmospheric sulfuric acid concentrations, Atmos. Chem. Phys., 13, 3865–3879, doi: 10.5194/acp-13-3865-2013, 2013.

Carslaw, N.: A new detailed chemical model for indoor air pollution, Atmos. Environ., 41, 1164–1179, doi: 10.1016/j.atmosenv.2006.09.038, 2007.

Fan, H., Zhao, C. F., and Yang, Y. K.: A comprehensive analysis of the spatio-temporal variation of urban air pollution in China during 2014–2018, Atmos. Environ., 220, 117066, doi: 10.1016/j.atmosenv.2019.117066, 2020.

Gong, Y. W., Chen, Z. M., and Li, H.: The oxidation regime and SOA composition in limonene ozonolysis: roles of different double bonds, radicals, and water, Atmos. Chem. Phys., 18, 15105–15123, doi: 10.5194/acp-18-15105-2018, 2018.

Hasson, A. S., Ho, A. W., Kuwata, K. T., and Paulson, S. E.: Production of stabilized Criegee intermediates and peroxides in the gas phase ozonolysis of alkenes: 2. Asymmetric and biogenic alkenes, J. Geophys. Res., 106, 34143–34153, doi: 10.1029/2001JD000598, 2001.

Lawrence, A. J. and Khan, T.: Indoor air quality assessment as related to household conditions in rural houses during winter season, Environ. Contam., 28, 221–244, doi: 10.1007/978-981-10-7332-8_11, 2017.

Lee, S. and Kamens, R. M.: Particle nucleation from the reaction of α-pinene and O_3, Atmos. Environ., 39, 6822–6832, doi: 10.1016/j.atmosenv.2005.07.062, 2005.

Paralovo, S. L., Barbosa, C. G. G., Carneiro, I. P. S., Kurzlop, P., Borillo, G. C., Schiochet, M. F. C., Godoi, A. F. L., Yamamoto, C. I., Souza, R. A. F., Andreli, R. V., Ribeiro. I. O., Manzi, A. O., Kourtchev, I., Bustillos, J. O. V., Martin, S. T., and Godoi, R. H. M.: Observations of particulate matter, NO_2, SO_2, O_3, H_2S and selected VOCs at a semi-urban environment in the Amazon region, Sci. Total Environ., 650, 996–1006, doi: 10.1016/j.scitotenv.2018.09.073, 2019.

Ravishankara, A. R.: Heterogeneous and multiphase chemistry in troposphere, Science, 276, 1058–1065, doi: 10.1126/science.276.5315.1058, 1997.

Sander, R.: Compilation of Henry's law constants (version 4.0) for water as solvent, Atmos. Chem. Phys., 15, 4399–4981, doi: 10.5194/acp-15-4399-2015, 2015.

Winterhalter, R., Neeb, P., Grossmann, D., Kolloff, A., Horie, O., and Moortgat, G.: Products and mechanism of the gas phase reaction of ozone with β-pinene, J. Atmos. Chem., 35, 165–197, doi: 10.1023/A:1006257800929, 2000.

Witkowski, B., Al-sharafi, M., and Gierczak, T.: Kinetics of limonene secondary organic aerosol oxidation in the aqueous phase, Environ. Sci. Technol., 52, 11583−11590, doi: 10.1021/acs.est.8b02516, 2018a.

Witkowski, B., Jurdana, S., and Gierczak, T.: Limononic acid oxidation by hydroxyl radicals and ozone in the aqueous phase, Environ. Sci. Technol., 52, 3402−3411, doi: 10.1021/acs.est.7b04867, 2018b.

Table S1. Wall loss fractions of SOA mass concentration at different relative humidity (RH).

RH	<0.5%	10%	20%	30%	40%	50%	60%	70%	80%	90%
Wall loss fraction (%)	7.21 ±0.72	6.57 ±0.77	6.88 ±0.82	7.02 ±0.93	7.65 ±0.95	8.21 ±0.88	11.29 ±0.90	13.04 ±1.21	15.67 ±1.16	17.10 ±1.45

Table S2. The amounts of SCIs (molecule cm^{-3}) under different concentrations of acetic acid (AA, molecule cm^{-3}) and different relative humidity (RH) in the first-generation oxidation.

RH / AA	< 0.5%	10%	40%	60%	80%
0.00	2.66×10^{11}	1.84×10^{11}	1.45×10^{11}	1.38×10^{11}	1.21×10^{11}
5.90×10^{11}	1.85×10^{11}	1.66×10^{11}	1.38×10^{11}	1.27×10^{11}	1.19×10^{11}
1.18×10^{12}	1.16×10^{11}	1.03×10^{11}	8.30×10^{10}	9.81×10^{10}	9.01×10^{10}
2.36×10^{12}	6.94×10^{10}	6.29×10^{10}	6.10×10^{10}	6.41×10^{10}	6.04×10^{10}
3.54×10^{12}	5.17×10^{10}	4.16×10^{10}	2.56×10^{10}	5.24×10^{10}	4.35×10^{10}
4.72×10^{12}	2.80×10^{10}	1.65×10^{10}	1.19×10^{10}	2.74×10^{10}	2.90×10^{10}
5.90×10^{12}	1.21×10^{10}	4.57×10^{9}	3.82×10^{9}	1.39×10^{10}	1.93×10^{10}
7.08×10^{12}	2.95×10^{9}	2.26×10^{9}	-2.58×10^{9}	-2.22×10^{9}	7.73×10^{9}
8.27×10^{12}	1.23×10^{9}	1.83×10^{9}	-5.57×10^{9}	1.28×10^{9}	5.31×10^{9}
9.45×10^{12}	-1.97×10^{9}	1.89×10^{9}	-3.52×10^{9}	3.69×10^{9}	3.55×10^{9}
1.06×10^{13}	2.46×10^{9}	1.78×10^{9}	-5.45×10^{8}	3.25×10^{9}	5.09×10^{9}
1.18×10^{13}	-4.92×10^{8}	-9.65×10^{8}	-4.40×10^{8}	3.85×10^{9}	5.55×10^{9}

Note: The negative values appearing in the table were caused by the errors of measurements under high AA concentration.

Table S3. The amounts of SCIs (molecule cm^{-3}) under different concentrations of acetic acid (AA, molecule cm^{-3}) and different relative humidity (RH) in the second-generation oxidation.

RH / AA	< 0.5%	10%	40%	60%	80%
0.00	2.21×10^{11}	1.60×10^{11}	1.29×10^{11}	1.65×10^{11}	2.41×10^{11}
5.90×10^{11}	1.45×10^{11}	1.38×10^{11}	1.13×10^{11}	1.12×10^{11}	1.77×10^{11}
1.18×10^{12}	1.01×10^{11}	1.02×10^{11}	8.79×10^{10}	9.10×10^{10}	1.09×10^{11}
2.36×10^{12}	6.05×10^{10}	5.33×10^{10}	6.16×10^{10}	6.13×10^{10}	7.84×10^{10}
3.54×10^{12}	5.49×10^{10}	4.50×10^{10}	5.54×10^{10}	5.47×10^{10}	4.68×10^{10}
4.72×10^{12}	4.75×10^{10}	4.49×10^{10}	4.61×10^{10}	4.79×10^{10}	2.86×10^{10}
5.90×10^{12}	3.84×10^{10}	2.98×10^{10}	3.79×10^{10}	2.55×10^{10}	1.49×10^{10}
7.08×10^{12}	1.97×10^{10}	1.91×10^{10}	2.88×10^{10}	2.24×10^{10}	1.21×10^{10}
8.27×10^{12}	1.21×10^{10}	9.06×10^{9}	1.94×10^{10}	2.16×10^{10}	1.03×10^{10}
9.45×10^{12}	9.84×10^{8}	6.89×10^{9}	1.38×10^{10}	1.85×10^{10}	1.01×10^{10}
1.06×10^{13}	-2.46×10^{8}	1.10×10^{9}	1.31×10^{10}	1.74×10^{10}	1.05×10^{10}
1.18×10^{13}	-2.46×10^{8}	9.78×10^{8}	1.24×10^{10}	1.77×10^{10}	1.03×10^{10}

Note: The negative values appearing in the table were caused by the errors of measurements under high AA concentration.

Table S4. The reactants concentrations (ppbv) in calculations of steady-state concentrations of SCIs in forest, urban area, and indoor area.

	Limonene	O_3	SO_2	NO_2
Forest	0.18	45	1[1]	2[2]
Urban area	0.15	45	10[3]	17[4]
Indoor area	2	20	10[5]	17[6]

[1] Boy et al., 2013; Paralovo et al., 2019

[2] Paralovo et al., 2019

[3] Fan et al., 2020

[4] Fan et al., 2020

[5] Lawrence and Khan, 2017

[6] Carslaw, 2007
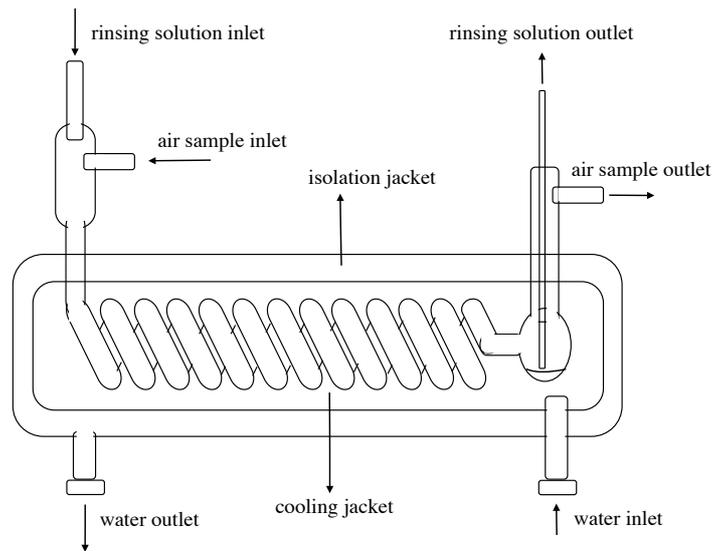
Figure S1. Diagram of the thermostatic coil collector.
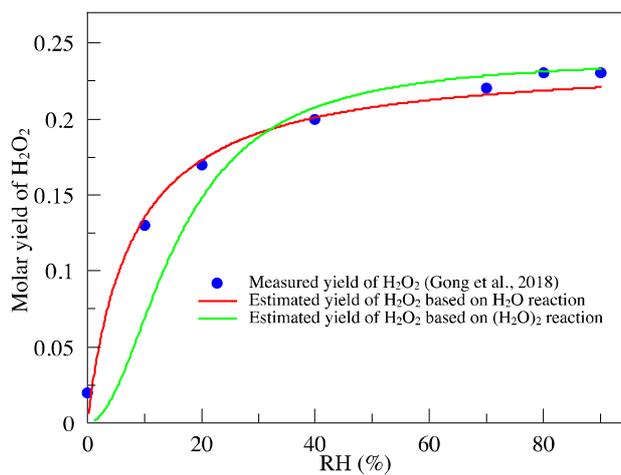
Figure S2. The dependence of the molar yield of hydrogen peroxide (H_2O_2) on relative humidity (RH). Blue dots: the measured yield of H_2O_2; Red line: the estimated yield of H_2O_2 based on SCI_I reaction with H_2O; Green line: the estimated yield of H_2O_2 based on SCI_I reaction with $(H_2O)_2$.
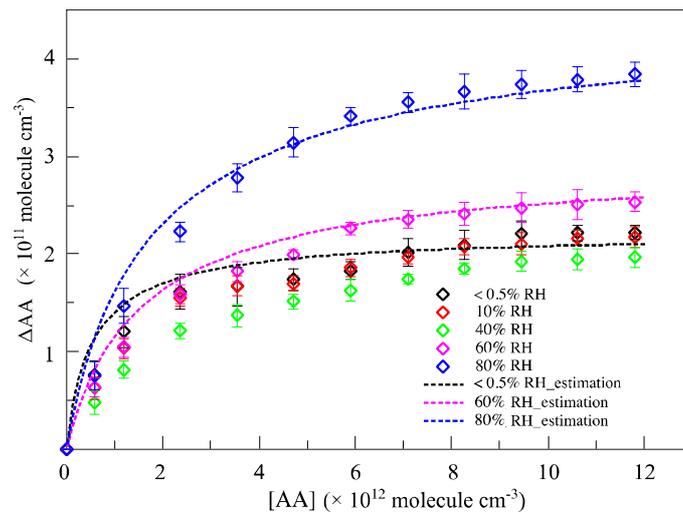
Figure S3. The variation of the consumption of acetic acid (ΔAA) with the concentration of acetic acid ([AA]) at different relative humidity (RH) in the second-generation oxidation. Scatters: measured ΔAA; Black line: estimated ΔAA at < 0.5% RH; Pink line: estimated ΔAA at 60% RH; Blue line: estimated ΔAA at 80% RH.
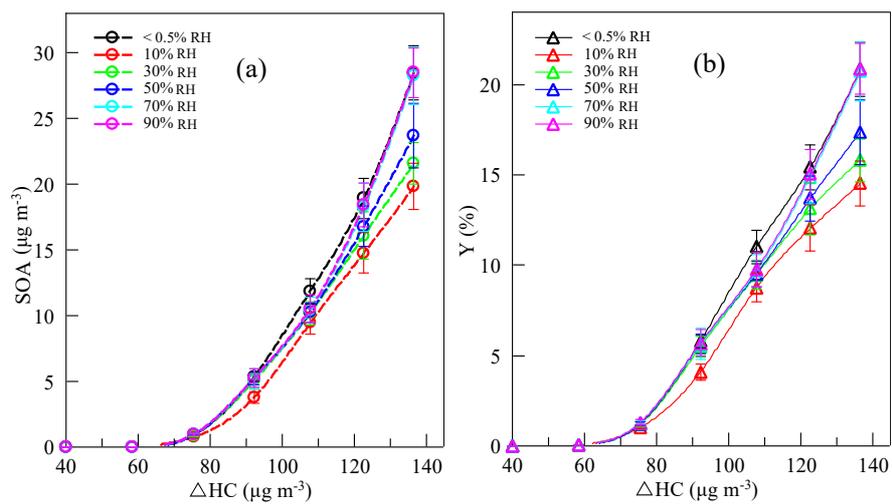
Figure S4. Growth curves of (a) SOA mass concentration (SOA) and (b) SOA yield (Y) versus limonene reacted (△HC) at different relative humidity (RH) in the first-generation oxidation.

Figure S5. Growth curves of (a) SOA mass concentration (SOA) and (b) SOA yield

(Y) versus reaction time at different relative humidity (RH) in the second-generation

oxidation.

Figure S6. The variation of SOA mass concentration (SOA) with the concentration of acetic acid ([AA]) at different relative humidity (RH) in the second-generation oxidation.